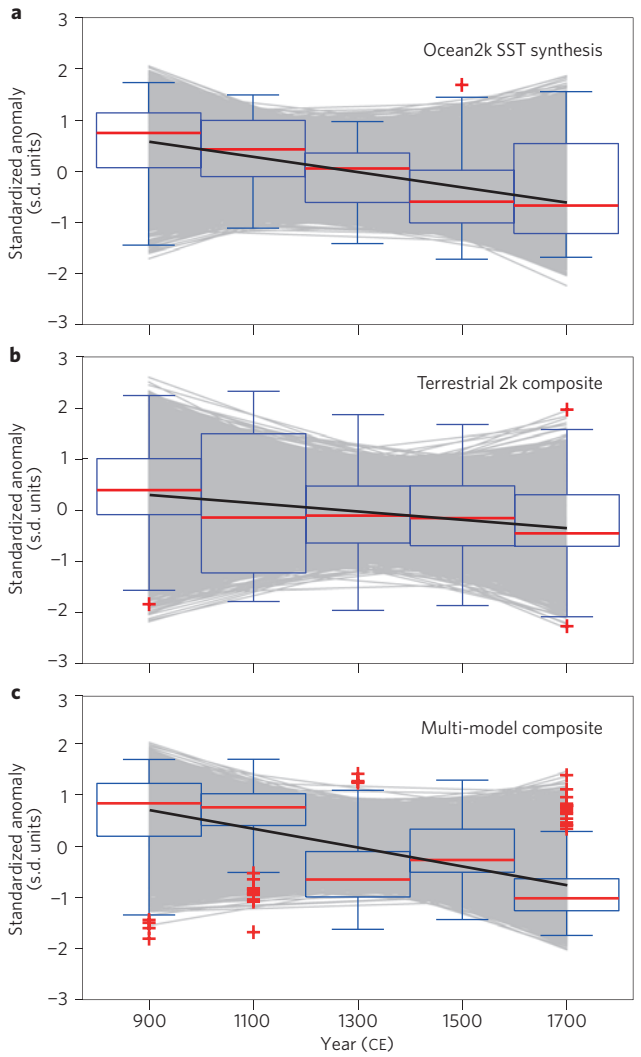

Figure 3 | Global SST and temperature trends for 801–1800 CE. a, Ocean2k SST synthesis (Fig. 2a). **b**, Terrestrial 2k composite (Supplementary Section 9). **c**, Multi-model composite, at the locations and periods for reconstructions in **a** (Methods; Supplementary Table S4). Box plots show 25th to 75th percentile range (blue boxes), median (red lines) and outliers (red crosses) to approximately 99.3% of the data range (blue 'whiskers') assuming normally distributed bin contents (Supplementary Table S14). Distribution (grey lines) and median (black line) of 10,000 Monte Carlo trend estimates are displayed for each synthesis. Trends are qualitatively similar between data and model composites.

for the 801–1800 CE interval is 85% and 73%, respectively (Methods; Supplementary Table S14). Although some of this agreement presumably arises from the proximity of the marine margins to land, the consistency of the Ocean2k SST synthesis and the Terrestrial 2k composite trends is probably due to a relatively coherent response to a common forcing on bicentennial timescales.

We also composite SST from six PMIP3-compliant simulations driven with realistic natural and anthropogenic forcings, matched to the same locations, time intervals and seasonality as the 57 Ocean2k reconstructions (multi-model composite; Fig. 3; Methods). The multi-model composite is also qualitatively consistent with the Ocean2k SST synthesis and has a higher (92%) probability of a cooling trend, albeit defined by a pronounced comparatively cold 1200–1400 CE bin. The qualitatively similar cooling trends in the Ocean2k SST synthesis and the multi-model composite are not an artefact of the standardization method (see Supplementary Section 4) and suggest that we may analyse the simulations to infer the mechanisms most likely to explain the palaeoclimate data.

External forcing of the global SST cooling

We isolate the forcing, or combination of forcings, most qualitatively consistent with the Ocean2k SST cooling trend observed for the past thousand years (the interval of common overlap) using two models from our multi-model composite (Fig. 4): SST simulated by the Commonwealth Scientific and Industrial Research Organisation (CSIRO) Mk3L model[26], run with the cumulative addition of orbital (O), greenhouse gas (G), solar (S) and volcanic (V) forcings; and by the LOVECLIM model[27], run with individual forcings as for CSIRO Mk3L, plus land-use forcing (L) and with all forcings (All). These simulations were matched to the 57 Ocean2k reconstructions (Methods). The CSIRO Mk3L simulations[26] suggest that OGS forcings combined give rise to only a weak and non-significant cooling trend, and are insufficient to explain the long-term Ocean2k global SST cooling trend (Fig. 4a; Supplementary Table S14). The LOVECLIM simulations[27], run individually with O, G, or S forcings, consistently show that these forcings do not explain the Ocean2k SST cooling trend (Fig. 4b; Supplementary Table S14).

The modest effect of greenhouse gases in generating a global ocean surface cooling trend in the model simulations is likely because greenhouse gas forcing is small prior to 1800 CE (Supplementary Fig. S4). Similarly, the magnitude of solar forcing, although uncertain[6,28,29], is small and does not generate a significant long-term cooling trend in the model simulations. Our analysis, however, cannot rule out regional and global mechanisms in which solar activity forces climate change on decadal to centennial timescales[30,31].

The single and cumulatively forced model simulations suggest that orbital forcing has only a minor role in generating a global SST cooling trend for the 801–1800 CE interval. Orbital forcing is associated with changes in insolation that are strongly dependent on the season and latitude[32], and over the Pleistocene epoch, orbital changes forced global climate through amplification mechanisms at high northern latitudes, including the well-known ice-albedo amplification[33]. High northern latitude temperature trends during the past millennium[27,34,35] have also been attributed to orbital forcing, specifically to declining high northern latitude summer insolation, amplified by feedbacks in the Arctic region and resulting in cooling[34,35]. However, when integrated over the full calendar year and spatially across the globe[32], the 1–2000 CE change in orbital radiative forcing at the top of the atmosphere is only $+4.4 \times 10^{-3}$ W m^{-2} (ref. 34). Consequently, the CSIRO Mk3L and LOVECLIM models both give weak and non-significant global ocean SST trends for the orbital forcing simulations, because the global ocean integrates the average global orbital forcing.

We find that volcanic forcing in CSIRO Mk3L, and volcanic and land-use forcings in LOVECLIM, produce a cooling trend most consistent with the Ocean2k SST synthesis (Fig. 4). The role of land-use change in forcing the Ocean2k SST cooling trend in the LOVECLIM simulation (Fig. 4b) arises from the increase in surface albedo owing to deforestation, inducing a net negative radiative forcing on land. The associated cooling is only partly compensated for by the reduced latent heat flux from lower summer evapotranspiration, resulting in overall cooling on land that is transmitted globally by the atmospheric circulation[27,36,37]. However, there are large uncertainties in our understanding of land-use forcing back in time, and with the simulated effects of land-use change on radiative forcing and the hydrological cycle[36,38,39].

Volcanic forcing

The influence of volcanic forcing on driving the SST cooling trend for the past millennium is surprising, as this forcing, although large, is relatively episodic[40,41]. The dominance of volcanic forcing

© 2015 Macmillan Publishers Limited. All rights reserved

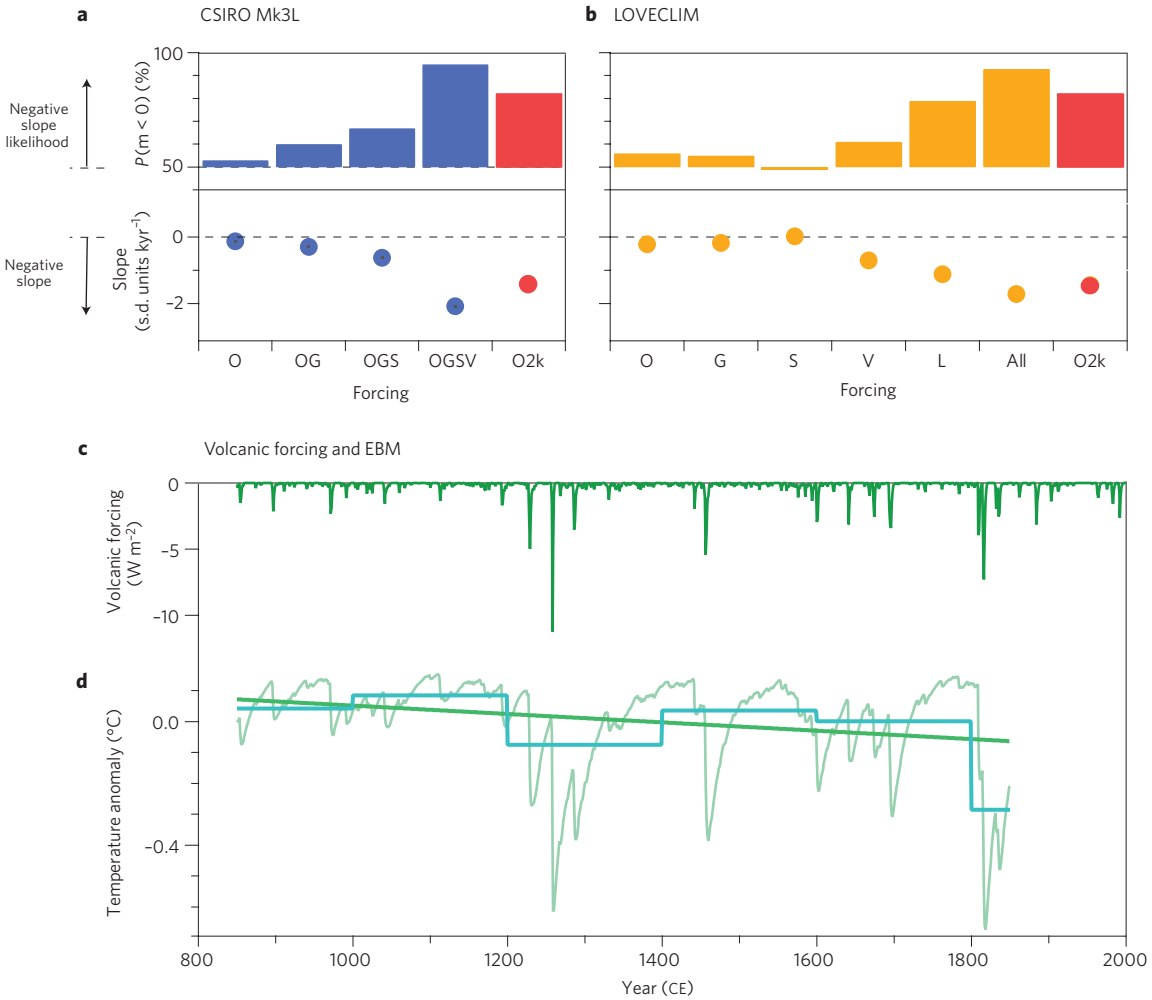

Figure 4 | Common Era Ocean2k SST synthesis and model simulation slopes, volcanic forcing and EBM response. a, CSIRO Mk3L simulations (blue). **b**, LOVECLIM simulations (yellow). Monte Carlo slopes (circles) and negative slope probabilities (bars; $P = 50\%$: equal probability of positive or negative slope; Methods). Ocean2k SST synthesis is also shown (O2k; red). Slope ± 2 s.e.m. values are smaller than the symbols. Time series in Supplementary Fig. S11. **c**,**d**, Volcanic forcing[6] (**c**) and EBM (**d**)temperature response (aqua line). 200-yr bin averages (blue lines) and linear fit (straight line) are shown. Volcanic forcing contributes to the cooling trend via a thermodynamic response.

over the 801–1800 CE interval may arise from increased volcanic event frequency and the occurrence of very large events early in the past millennium, and/or internal amplification of volcanic forcing within the climate system[6,42–44] (Supplementary Fig. S4). In particular, large volcanic eruptions between 1150 and 1300 CE, and again during the early fifteenth century, may be responsible for the observed cooling[43,45].

We use an energy balance model[46] (EBM; Supplementary Section 10) to simulate the thermodynamic response of a mixed-layer ocean to the volcanic radiative forcing (Fig. 4). The EBM results do not fully match the bin-to-bin changes in the Ocean2k SST synthesis, probably because internal variability is absent in the EBM, there are contributions from other forcings and the EBM has a weak long-term memory (it contains no deep-ocean coupling). However, we find that the radiative change from repeated clustering of volcanic eruptions over the past millennium by itself is sufficient to explain a long-term cooling trend. This suggests that the Ocean2k SST cooling trend, at least for >200-yr timescales, might simply represent a first-order thermodynamic response to stochastic volcanic forcing that increased in frequency from the early to late past millennium. A comparison of Northern Hemisphere reconstructed temperatures with a volcanically forced upwelling–diffusion EBM reached a similar conclusion[47].

Nonetheless, several dynamical mechanisms have been proposed to explain an amplified ocean response to the volcanic forcing during the past millennium[43,48,49]. Specifically, on decadal timescales the volcanic eruptions could have induced a fast cooling in the tropics, leading to anomalously high pressure over the continents that reduced Atlantic Ocean trade wind stress curl anomalies[49]. The subsequent ocean adjustment propagated the cooling to the high latitudes and, over time, weakened the Atlantic meridional overturning circulation (AMOC), resulting in sea ice expansion. On centennial timescales, eruptions are thought to have reduced downwelling shortwave radiation, increased surface albedo and led to lower elevation snowlines in regions north of 60° N (refs 43,48). The associated cooling and increase in sea ice extent further amplified Arctic and North Atlantic cooling[43,48]. Open ocean convection may have declined, weakening the AMOC and its associated ocean heat transport to the high-latitude North Atlantic[48]. In turn, the reduced AMOC may have reduced sea ice melt, permitting sea ice to persist for a century, thus perpetuating the initial cooling induced by the frequent eruptions in the late thirteenth century[43,48]. These model results suggest that dynamical mechanisms might transform increases in frequency of volcanic eruptions into a longer term cooling.

We test for changes in AMOC both in the volcanic-only forcing LOVECLIM simulation and in the orbital–greenhouse

© 2015 Macmillan Publishers Limited. All rights reserved

Methods

SST data. The Ocean2k SST synthesis is based on 57 peer-reviewed, publicly available reconstructions solely from marine archives (Fig. 1; Supplementary Table S1) and listed in the Past Global Changes Ocean2k metadatabase (http://pages-igbp.org/ini/wg/ocean2k/intro). Reconstructions are expected to record SST and have a chronology anchored by at least two ages, within error, between 200 yr before the CE (BCE) and present. Only data between the oldest and youngest dates were used (see Supplementary Section 1 for additional details). Ages were converted to the CE/BCE timescale and SST calibrations from the original publications were used.

Models. Climate simulations available from 850 CE were selected from the BCC-CSM1-1, CCSM4, FGOALS-s2, LOVECLIM and MPI-ESM models, and available from 801 CE from the CSIRO Mk3L model (see Supplementary Section 2 for references). The model forcings follow the Coupled Model Intercomparison Project Phase 5 (CMIP5)/PMIP3 protocol[6]. For this subset of simulations there is no significant drift owing to experimental design[24]. Model output was truncated at 1800 CE to focus on the pre-industrial past millennium. For Fig. 4, additional LOVECLIM and CSIRO Mk3L simulations were used, driven by only selected forcings (Supplementary Section 2; Supplementary Table S4; Supplementary Fig. S11). EBM details are in Supplementary Section 10. The model simulation time series in Figs 3 and 4 are from the same location (or, if a margin site, the nearest straight-line distance grid box), time interval and season as the 57 SST reconstructions. See Supplementary Section 5 for details on Fig. 1 construction.

Binning and standardization. Data from each of the 57 reconstructions were averaged into 200-yr bins, to give 10 bins, centred on 100, 300 CE and so on, up to 1900 CE. Each binned series was then standardized by its average and standard deviation. The Ocean2k synthesis trends are insensitive to bin centre placement (Supplementary Section 5; Supplementary Fig. S5). The mean of the age distribution of individual data points within each bin is very close to the bin centre (Supplementary Table S5). The binned and standardized values are then treated as a sample of the SST population within each bin, with age uncertainty approximately equal to bin width. The numbers of chronological control points per bin are in Supplementary Fig. S1. Slope and slope probabilities were estimated using Monte Carlo simulations (below). Our results are insensitive to standardization (Supplementary Section 4). All simulated SSTs were binned and composited as described here.

Sensitivity tests. Sensitivity tests were carried out on the Ocean2k synthesis cooling trend to assess the influence of (Supplementary Table S1): (1) reconstruction type, for example, alkenone, foraminiferal Mg/Ca, other (microfossil transfer functions or modern analogue technique, TEX_{86} and coral Sr/Ca); (2) response seasonality (mean annual, warm, cool); (3) number of ^{14}C dates/reconstruction (>4 or ≤4 ^{14}C dates; note, four reconstructions were not ^{14}C dated and are not included in this test (Supplementary Table S1)); (4) sampling resolution (<8, ≥8 samples per bin); (5) sedimentation rate (≤0.1cm yr^{-1}, >0.1 cm yr^{-1}); (6) water depth (>500 m, <500 m); (7) basin (Arctic, Atlantic, Indian, Mediterranean, Pacific, Southern); (8) latitude (extratropical Northern Hemisphere (>30° N), tropical (30° N–30° S), extratropical Southern Hemisphere (>30° S)); (9) hemisphere (northern or southern); and (10) locations within pre-defined upwelling zones (Supplementary Table S3). The sub-data sets were binned, standardized and composited as per the Ocean2k synthesis. Medians are plotted in Fig. 2b. We use water depth as a proxy for open ocean conditions (Supplementary Section 6). Maps of each sensitivity analysis (Supplementary Fig. S9) were generated to examine the potential spatial bias associated with each characteristic.

Each bin value (in each sensitivity test) represents a standardized mean of up to 57 data points per 200-yr bin, and the full 2-kyr data set includes 10 standard deviations (one value per bin). Therefore, to represent the overall error for each sensitivity analysis, a median standard deviation for the 10 bins was calculated, and is plotted in the error histograms (Fig. 2b, right).

Slope calculations. Slopes and slope probabilities were estimated from Monte Carlo simulations. Ten thousand linear least-squares fits were estimated; for each realization, a single observation from each bin of a given synthesis was randomly selected (with replacement) to create the fit estimate. The median slope of these fits was then calculated. Slopes were similarly estimated for the Ocean2k synthesis (Figs 2–4), Terrestrial 2k and multi-model composites (Fig. 3), and single and cumulative forcing model SST estimates (Fig. 4; Supplementary Fig. S11). Slopes in Fig. 4 are plotted with $\pm$2 s.e.m., assuming a normally distributed sample of the regression slope.

Data availability. Data URLs for the 57 reconstructions are in Supplementary Table S2. Ocean2k SST synthesis data matrix and metadata are at http://www.ncdc.noaa.gov/paleo/study/18718. Model simulation URLs are in Supplementary Table S4. Terrestrial 2k composite data are at https://www.ncdc.noaa.gov/cdo/f?p=519:2:0::::P1_study_id:12621 and update 1.1.1 at http://dx.doi.org/10.6084/m9.figshare.1054736.

Code availability. Compositing code used to generate the Ocean2k SST synthesis (Fig. 2a) is at http://www.ncdc.noaa.gov/paleo/study/18718.

© 2015 Macmillan Publishers Limited. All rights reserved